Original scientific paper

https://doi.org/10.33180/InfMIDEM2025.403

Informacije MIDEM
Journal of Microelectronics,
Electronic Components and Materials
Vol. 55, No. 4(2025), XX – XX

A Wireless Optical Gate and IMU System for Agility Assessment: Architecture, Synchronization and Validation

Anton Kos, Erik Keš, Matevž Hribernik, Sašo Tomažič, Anton Umek

Faculty of Electrical Engineering, University of Ljubljana, Ljubljana, Slovenia

Abstract: Accurate, field-ready timing and motion capture are essential for assessing agility beyond the limits of manual stopwatches. We present a modular measurement system that fuses infrared (IR) optical gates for robust event detection with a trunk-worn inertial measurement unit (IMU) for kinematic profiling. Each sensing node is built on an Adafruit Feather M0 Wi-Fi microcontroller and communicates via UDP to a laptop server. Time alignment is accomplished without internet connectivity: the server establishes a relative epoch and executes a triple-handshake broadcast protocol, while timestamps are generated at the edge to avoid latency bias from transport or processing. Module- and device-level characterization shows that IR-receiver processing combined with interrupt service routine latency yields a per-event timestamp error of 0.54 ms ± 0.14 ms (latency ± uncertainty), and local clocks remain stable over the durations relevant to agility trials. In wireless operation, accepted synchronization attempts form tight response clusters in favorable RF conditions, whereas congested environments may require retries; for section times across different gates we therefore report a conservative inter-node uncertainty. End-to-end validation across laboratory, entry-hall, and gym venues using the Agility T-test confirms that total test time measured on the same start/finish gate remains below 1 ms error over 10–20 s trials. Synchronized IMU waveforms add explanatory value beyond total and split times by revealing braking, change-of-direction, and re-acceleration phases. The system provides a deployable workflow with substantially improved precision over manual timing. Future work will target more robust synchronization and expanded analytics, including automated phase detection, asymmetry indices, and optional integration with indoor positioning.

Keywords: infrared gates; IMU; embedded systems; wearable sensor device; wireless synchronization; agility testing

Brezžični sistem za ocenjevanje agilnosti na osnovi optičnih vrat in kinematičnih senzorjev: arhitektura, sinhronizacija in validacija

Izvleček: Natančno merjenje časa in zajem gibanja na terenu sta ključna za ocenjevanje agilnosti onkraj omejitev ročnih štoparic. Predstavljamo nizkocenovni, modularni merilni sistem, ki združuje infrardeča (IR) optična vrata za robustno zaznavanje dogodkov in na trupu nameščeni inercialni merilni senzor (IMU) za kinematično profiliranje. Vsako merilno vozlišče temelji na mikrokrmilniku Adafruit Feather M0 Wi-Fi in z uporabo UDP komunicira s strežnikom na prenosniku. Časovno uskladitev izvedemo brez internetne povezave: strežnik vzpostavi relativno epoho in izvede oddajni protokol s trojnim rokovanjem, medtem ko se časovni žigi tvorijo na robu sistema (na napravi), da se izognemo pristranskosti zaradi zakasnitev prenosa ali obdelave. Karakterizacija na ravni modulov in naprav pokaže, da kombinacija obdelave v IR sprejemniku in zakasnitve prekinitvene rutine prinese napako časovnega žiga na dogodek 0.54 ms ± 0.14 ms (zakasnitev ± negotovost), lokalne ure pa ostanejo stabilne v časovnih intervalih, pomembnih za preizkuse agilnosti. Pri brezžičnem delovanju sprejeti poskusi sinhronizacije v ugodnih RF-razmerah tvorijo tesne skupke odzivov, medtem ko v zasičenih okoljih lahko zahtevajo ponovitve; zato pri časih odsekov med različnimi vrati navajamo večjo negotovost. Celovita validacija v laboratoriju, avli in telovadnici z uporabo T-testa agilnosti potrjuje, da ima skupni čas testa, izmerjen na istih začetnih/končnih vratih, napako manjšo od 1 ms pri poskusih, dolgih 10–20 s. Sinhronizirani IMU signali dodajo pojasnjevalno vrednost onkraj skupnih in delnih časov, saj razkrivajo faze zaviranja, menjave smeri in ponovne pospešitve. Sistem omogoča enostavno uvedljiv potek dela z bistveno izboljšano natančnostjo v primerjavi z ročnim merjenjem. V prihodnje načrtujemo še zanesljivejšo sinhronizacijo in razširjeno analitiko, vključno s samodejnim zaznavanjem faz, indeksi asimetrije ter po potrebi integracijo s pozicioniranjem v zaprtih prostorih.

Ključne besede: infrardeča vrata; IMU; vgrajeni sistemi; nosljiva senzorska naprava; brezžična sinhronizacija; testiranje agilnosti

* *Corresponding Author's e-mail: anton.kos@fe.uni-lj.si, anton.umek@fe.uni-lj.si*

1 Introduction

Time–motion tests, especially change-of-direction (COD) tasks, remain a staple of field-based performance assessment because they are simple to administer and show good reliability and construct validity across sporting populations [1]. One example of COD task is T-test studied in this work. However, manual timing introduces human start and stop reaction latency and split-time variability when compared with electronic solutions [2]. Infrared (IR) timing gates and photoelectric cells help reduce operator delay, but their accuracy can still be affected by several factors. Athlete posture (e.g., knee or arm swing), beam geometry, and starting procedures can interfere with triggering, and performance also differs between single- and dual-beam configurations. Recent systematic evidence further shows that commercial systems can produce significant offsets and are not universally comparable, particularly during the first 5–10 m of acceleration of the linear speed test [3].

In parallel, inertial measurement units (IMUs) have become a practical way to capture kinematics in environmentally valid settings. A 2021 scoping review concluded that IMUs can quantify COD performance, but highlighted heterogeneity of metrics and the need for rigorous validation in sport-specific tasks [4]. Newer studies have started to fill this gap: single-sensor wearables can segment COD and derive interpretable performance markers in the field [5]; multi-IMU systems can capture lower-limb kinematics with high sagittal-plane agreement to optoelectronic references, albeit with greater error in frontal and transverse planes [6], [7]; and foot-mounted IMUs show promising validity for velocity tracking in team sports [8]. There is also growing interest in combining IMUs with phone-based markerless methods to balance practicality and accuracy [9].

A persistent systems-engineering challenge is precise time alignment across distributed, wireless nodes so that timing-gate events and IMU signals are fused without drift. Energy-efficient clock discipline for Wi-Fi/IoT devices has been proposed (e.g., ecoSync) to trade synchronization accuracy for battery life in multi-sensor settings [10]. Precision Time Protocol (PTP) over Wi-Fi can reach microsecond-level accuracy with careful tuning/hardware support, but performance depends on network interface capabilities and timestamping paths [11], while Network Time Protocol (NTPv4) remains a robust baseline for general deployments [13]. When spatial context is needed (e.g., split timing plus trajectories), Ultra-Wideband (UWB) real-time locating systems are an established option for indoor positioning with high update rates and robustness to multipath [12].

Motivated by the lack of systems that provide synchronized timing gate events and IMU signals in real-world settings without Internet access, and aiming for a low-cost, hardware-independent solution, we present a wireless synchronized sensor system that integrates (i) IR gates for robust, low-latency location-bound event timing, (ii) body-worn IMUs for rich kinematic profiling, and (iii) a synchronization layer to ensure sub-frame timestamp coherence across nodes. Building on our prior engineering work that demonstrated millisecond-level timing accuracy at the device level [14], we target sports-relevant tasks (e.g., agility tests) where both total time and movement quality matter.

Our contributions are: (1) a low-cost, modular, field-deployable architecture that unifies IR-gate events and IMU streams under a common clock, (2) a synchronization strategy compatible with commodity Wi-Fi while remaining energy-aware, and (3) an analysis pipeline that provides both standard split times and additional kinematic micro-metrics of execution.

2 Background & Related Work

Timing technologies. Manual timing is convenient but systematically biased relative to electronic systems [2]. Photoelectric timing gates reduce operator error, but the height of the beam and the number of beams, the starting protocol and the morphology of the object affect the triggers and thus the measured times. A recent systematic review found that double-beam gates reduce false triggers more effectively than single-beam systems. It also reported that different systems are not always interchangeable, particularly in the early acceleration phase. This emphasizes the need to specify device models and setups in studies [3]. Recent validation studies characterize the differences between systems (e.g. Chronojump vs. Witty) and propose fitting equations for comparability [3].

Wearable sensing for agility tests. IMUs are widely used to capture movement quality alongside total time. The scoping review by Alanen et al. summarizes reliability/validity evidence and calls for standardized metrics in COD analysis [4]. Subsequent work shows that a single trunk-worn GNSS-IMU can decompose standard agility tests into interpretable phases [5], while laboratory-grade comparisons indicate high waveform agreement in the sagittal plane and task-/plane-dependent limitations elsewhere [6], [7]. Foot-mounted IMUs have been shown to provide valid measurements of velocity in team sports [8]. Early studies also suggest they can work well alongside modern phone-based markerless systems [9].

Clock synchronization and spatial context. Multi-sensor fusion in the field depends on stable sub-millisecond alignment. Energy-aware Wi-Fi synchronization (ecoSync) reduces overhead for battery-powered nodes [10]; PTP over Wi-Fi can reach ≈1 µs accuracy with careful engineering, though commodity hardware support is uneven [11], while NTPv4 remains a practical, standards-based baseline [13]. For positioning, UWB RTLS offers accurate, robust indoor tracking and is widely reviewed for real-time deployments [12].

Compared with timing-only protocols that report total or coarse split times and remain sensitive to beam setup and inter-system offsets [1]–[3], our approach

fuses robust IR-gate events with IMU signals under a common clock. This yields not only how much time was spent, but where and why within each section; IR gates also curb the segmentation uncertainty that affects IMU-only pipelines [4]–[9]. We further quantify the full error budget, per-device measurement error, local clock drift, and inter-node synchronization, so uncertainties propagate to both total and section-level metrics.

In our system, we implement lightweight Wi-Fi synchro-nization positioned between NTP (practically ms-level, but dependent on the network connection) and hardware-assisted PTP (µs-level, but less commodity-friendly) [10], [11], [13], along with edge timestamping, compact UDP transport, and a stable time base. In practice, this provides sub-ms device coherence and explicitly characterized uncertainty between nodes in congested RF environments. This results in a field-suitable workflow for agility testing with comparable times and explanatory IMU waveforms [3], [5]–[9]. Thus, our solution is comparable to NTP, but network independent, and although less accurate than PTP, it is independent of specific network interface functionalities.

3 Materials and Methods

3.1 System architecture

The system shown in Figure 1 comprises (1) distributed measurement nodes of two different types: IR timing gates and a wearable IMU unit, (2) a laptop server connected to (3) a Wi-Fi access point (AP). Nodes transmit ASCII-encoded UDP packets to the server; UDP was chosen to minimize head-of-line blocking and reduce latency from acknowledgments. As the system operates without connection to the internet, synchronization does not use NTP; instead, devices align to a relative time established by the server at a synchronization instant. Devices are uniquely identified and assigned roles (gate index, wearable) by the server before a trial.

3.2 Hardware

Microcontroller & radio. Each mobile node (IR timing gates and wearable IMU devices) uses an Adafruit Feather M0 Wi-Fi microcontroller board (SAMD21 + ATWINC1500) [15]–[17]. The AP used in development was a TP-Link Archer C7 (802.11b/g/n); the server is wired to the AP for stability and reduced radio use.

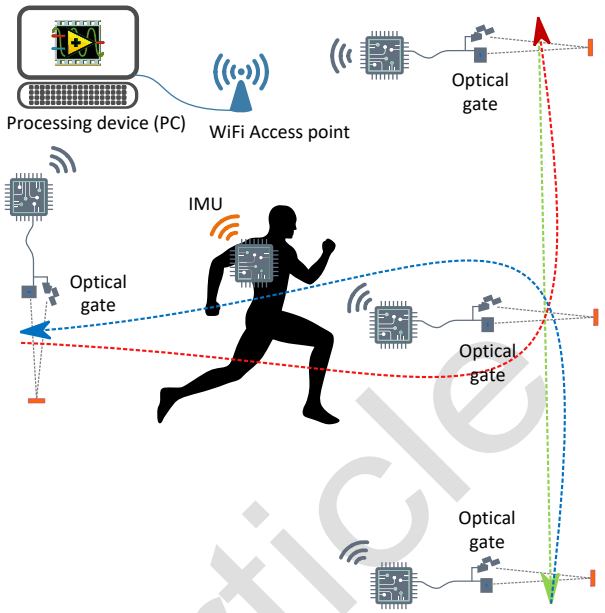

Figure 1 System architecture with a processing device (server), multiple IR optical gates, wearable IMU, Wi-Fi Access point. Configuration showing a T-test case.

IR timing gates. Gates consist of a 940 nm IR emitter and modulated receiver (IS471F), see Figure 2. The IS471F's data sheet specifies a 400–670 µs internal processing delay, i.e., an absolute uncertainty of up to ±135 µs around a ~535 µs mean [18].

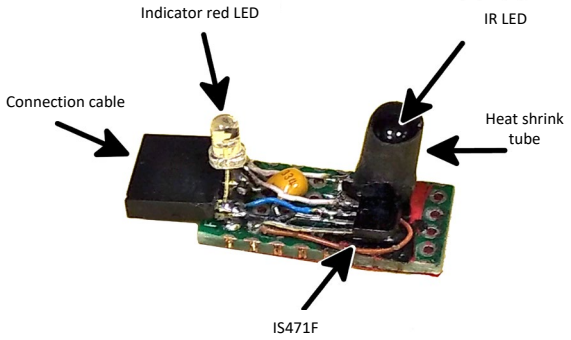

Figure 2 IR timing gates.

Wearable IMU. We used LSM6DS33 (accelerometer & gyroscope, set to ±16 g and ±2000 dps, 100 Hz) and BNO055 (orientation/acc/gyro/mag, 100 Hz) mounted at users' lower back, near the center of mass of the body. Logged channels, depending on a sensor, include fused orientation, linear acceleration (gravity-compensated), raw accelerometer/gyroscope, magnetometer, and battery voltage [21], [22].

3.3 Firmware and communication

Node operation. Gate crossings trigger interrupts that immediately store the local timestamp and raise a flag; packet assembly and transmission occur in the main loop to keep interrupt service routines (ISRs) minimal. IMU sampling follows a fixed-interval loop (read LSM →

read BNO → check send window → send). Both flows are implemented as lightweight state machines.

Server application. The LabVIEW program manages (1) synchronization exchanges, (2) receive loops for UDP, (3) role assignment and configuration, and (4) logging and live visualization. The code modules and GUI tabs for sync/config and packet reception are documented with block diagrams and front-panel screenshots [14].

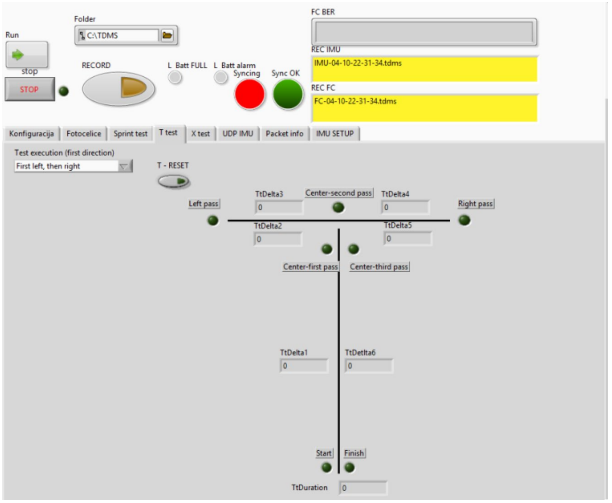

Figure 3 Appearance of the LabVIEW application graphical interface when performing a T-test.

3.4 Time measurement accuracy

During operation, the system's primary function is time measurement; either for event stamping or sensor sampling. Owing to imperfections, timing errors arise at both intra- and inter-device levels. We decompose the total timing error into: (a) electronics, (b) local clock drift, and (c) inter-node synchronization.

For intra-device outcomes, only (a) and (b) are relevant. A typical case is the total test time when the athlete starts and finishes at the same gate (as in our T-test); synchronization error is irrelevant because the result derives from timestamps produced by a single gate. For inter-device outcomes, e.g., partial (split) times between successive gates, component (c) is critical, since the result combines timestamps from different, imperfectly synchronized nodes.

Notably, processing and communication latencies do not bias timestamp accuracy. As illustrated in Figure 4, delays in the system stem from sensor device, microcontroller processing, communication, and the processing device. Only the first contributes to time-measurement error; the others affect overall system performance and are therefore not analyzed further in this paper.

Figure 4 Delay sources in the system.

3.5 Device synchronization

During system development, two synchronization methods were implemented: (a) wired and (b) wireless.

In the wired approach, all devices (optical gates or wearable sensors) are physically connected to a synchronization apparatus that provides a common trigger signal simultaneously, as shown schematically in Figure 5. This method is suitable when the test setup allows straightforward handling of optical gates and wearable sensors.

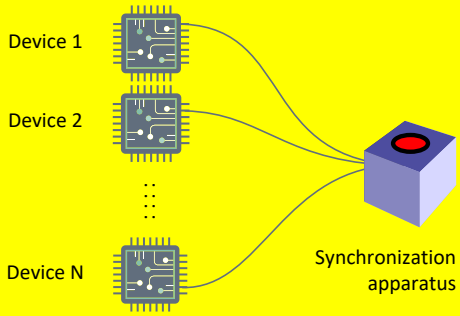

Figure 5 Wired synchronization scenario in which an apparatus drives the sync signal for gates/sensors.

In the wireless approach, the processing device broadcasts a Wi-Fi synchronization packet to all mobile nodes. This method is particularly advantageous when regular synchronization is needed but physical manipulation of the gates and/or wearable devices is impractical, or when time constraints limit access to athletes, as is often the case with elite teams. To address these scenarios, we developed and implemented a triple-handshake synchronization protocol:

- The server is configured with the number of microcontrollers in the system (*N*).
- Before each measurement, all microcontrollers wait for a synchronization packet.
- The server initiates synchronization by broadcasting a packet containing the current synchronization attempt index (0–9).
- Upon reception, each microcontroller records its current local time from system startup.
- Each microcontroller responds to the server with a packet that includes the synchronization attempt index.
- Once the server has received responses from all *N* nodes, it broadcasts a confirmation packet to conclude synchronization.
- Each microcontroller then stores the most recent recorded timestamp as t_0, which is used as the reference time for subsequent measurements.

The messages used in this protocol are defined as:

- TREQ-N: server synchronization request with attempt index *N*,
- TRESP-N: microcontroller response to synchronization attempt *N*,
- TSUCC: server broadcast confirming successful synchronization to all nodes.

Protocol diagrams for the server and device sides are shown in Figure 6. The server controls communication by sending TREQ and TSUCC messages based on the number of successfully received responses from the devices (TRESP) and any possible timeouts. If the maximum number of unsuccessful synchronization attempts is reached, synchronization ends and the user is notified. Some internal operations, such as setting the local time or advancing counters, are not shown in the diagram.

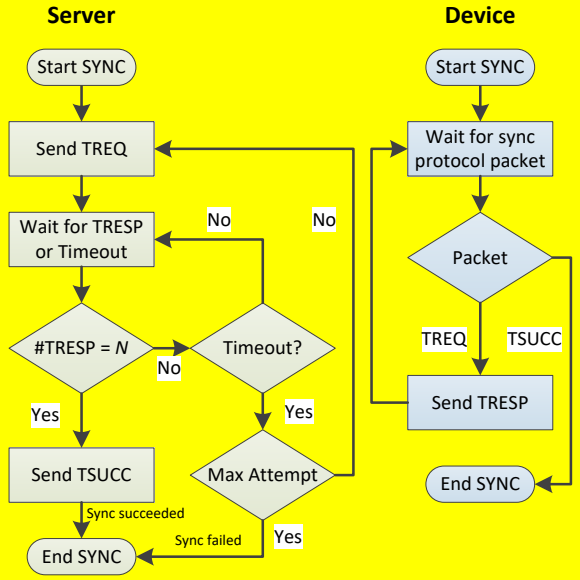

Figure 6 Server and device side protocol diagrams.

Figure 7 illustrates the synchronization process of an example system with four devices, showing one failed and one successful synchronization attempt. The initial synchronization request, TREQ-0, at time t_{r0} receives only three responses, TRESP-0, at the server, resulting in a failed attempt. After the protocol timeout, the next attempt, TREQ-1 at time t_{r1} succeeds, as all four responses TRESP-1 are received. The successful synchronization is communicated to the devices with the confirmation message TSUCC.

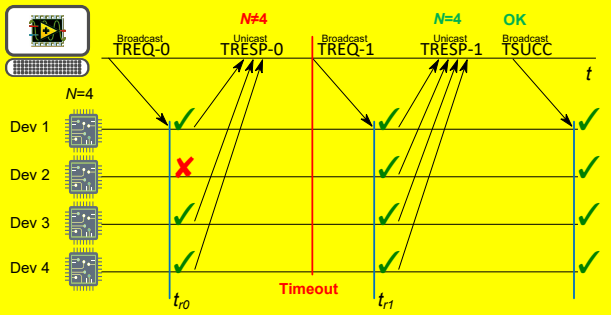

Figure 7 Triple-handshake synchronization protocol.

4 Results

The focus in this section is on time measurement and synchronization inaccuracies and not on the actual athletes' results of the performed agility tests.

4.1 Agility T-test

Agility T-test trials were conducted in three environments: the laboratory (device functionality testing), the faculty entry hall (initial system validation), and the gymnasium (real-world conditions). The configuration of optical gates for the left-side execution is shown in Figure 8. In this mode, the athlete turns left after the first passage through gate 2. Both IMUs were configured as described previously (LSM6DS33 at 100 Hz; BNO055 at 100 Hz). Field measurements outcomes are reported as split times and basic kinematic signals [14]. Detailed sport-science interpretation is planned in collaboration with domain experts.

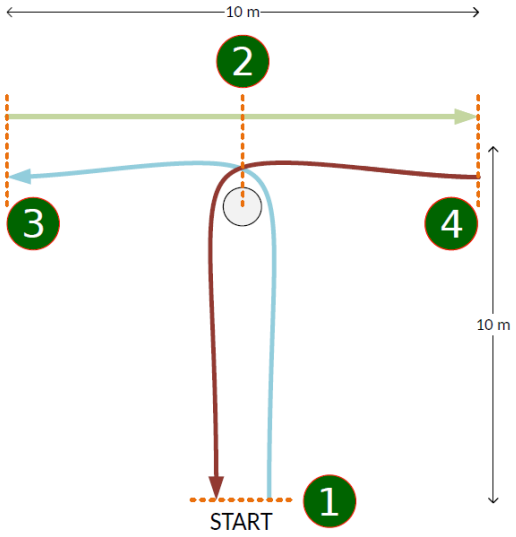

Figure 8 Setup of measurement gates for the T-test: green circles indicate the sequential numbering of gates for the left-side execution.

4.2 Device-level timing measurements

As noted in Section 3.2, the IS471F introduces an internal processing delay of 400–670 µs (mean ≈ 535 µs), yielding an absolute uncertainty of ± 135 µs as specified in the data sheet [18]. Digital toggling contributes < 100 ns and is therefore negligible [14]. Oscilloscope measurements show a constant ISR entry latency of ≈ 1.6 µs from input edge of the IR optical gate signal to the first MCU output transition (Figure 9). Together, the per-event timestamp at a gate is 536.6 ± 135 µs (mean latency ± uncertainty).

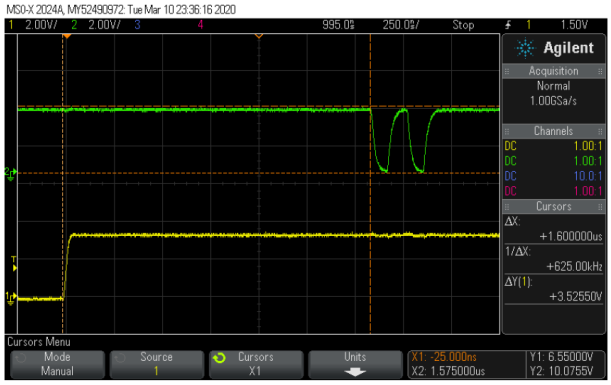

Figure 9 Oscilloscope screenshot of interrupt service routine latency measurement. The yellow trace shows the signal at the digital input, while the green trace represents the signal at the digital output of the microcontroller.

4.3 Microcontroller clock drift

When assessing timing performance, a fundamental question is whether the obtained results can be regarded as reliable. If the measurement clock exhibits excessive error, deviations may accumulate over longer intervals and exceed acceptable limits. To address this, we evaluated the clock accuracy of the microcontrollers used in our measurement system, which depends on quartz crystal tolerances.

As shown in Figure 10, four microcontrollers were tested. Following thermal stabilization, the devices were synchronized, and a series of measurement episodes was performed to monitor differences in recorded times relative to the initial synchronization. After approximately 400 s of operation, individual devices exhibited drift of up to ±2.5 ms, corresponding to about 6.25 µs/s. At this rate, a single microcontroller would accumulate a timing error of 1 ms in roughly 160 s, what is more than suitable for standard agility tests that generally do not last more than 20 s.

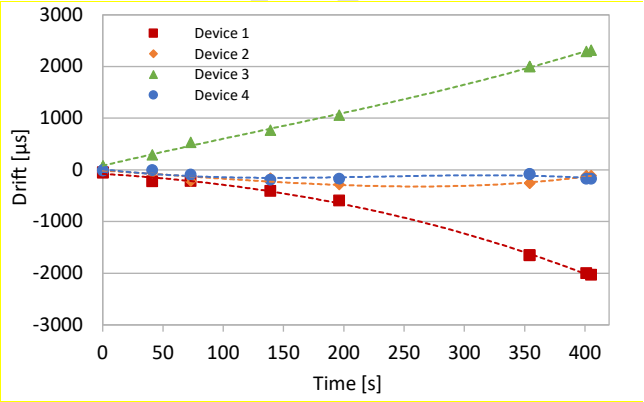

Figure 10 Deviation of microcontroller clocks within a 400 seconds interval relative to the average event time.

4.4 Synchronization error

Because the system is not connected to the internet, devices are not disciplined to absolute time. The server sends a synchronization request; devices record local times on receipt and reply, after which the server assigns a relative epoch and estimates offsets and rates per device.

In wired scenarios, synchronization errors are in the range of microseconds and are therefore negligible. In wireless scenarios, the errors can become much larger. By conducting measurements of the delay of the triple handshake protocol in different environments, we obtained these results. In favorable RF conditions (gym), the inter-device spread during sync was ≈45–55 µs. Under congested RF (faculty hall), sync quality degraded to several milliseconds and many retries were needed. Conservatively, we report an upper-bound system-level synchronization term of 15 ms ± 10 ms for inter-node section times. Unfavorable results can be improved via a dedicated radio channel [14].

4.5 End-to-end and section timing accuracy

Combining electronics delay, ISR latency, local drift and favorable synchronization, we can see that: (a) the error for total T-test time, which is of duration between 10 and 20 seconds, remains well below 1 ms, and (b) for section times spanning different gates we propagate the drift and sync terms alongside device-level error when reporting uncertainty. In favorable RF conditions the clock drift and synchronization error add less than 100 µs, while in unfavorable conditions the additional error can be up to 25 ms (conservatively).

4.6 System validation

We validated the system in stages: module, device, network, and end-to-end. We used procedures designed to mirror real use and to isolate each source of uncertainty reported in Sections 4.2–4.5.

Module level. To characterize sensing and stamping, we drove controlled interruptions of the IR beam and observed the signal path with an oscilloscope: IR receiver output → MCU interrupt pin → ISR entry marker (test firmware toggles a GPIO on ISR entry). This bench setup verified that timestamps are produced at the interrupt edge, that ISR handling is constant across repeats, and that transport/processing downstream (UDP, server logging) does not bias event times. The resulting timing budget is summarized in Section 4.2 and in Figure 9.

Device level. To evaluate clock stability independently of networking, four microcontrollers were wired in parallel to a common trigger that emulates an optical-gate event. After thermal stabilization and an initial sync, we issued repeated triggers at variable intervals and compared each node's recorded time to the run's reference trace. This procedure reveals relative drift and informs the practical re-synchronization policy used in trials (Figure 10).

System level. Wireless synchronization was exercised with the triple-handshake procedure (Figure 7). Before each trial, the server broadcast a sync request; nodes stamped local receipt time and replied; the server accepted the attempt only if responses formed a tight cluster (indicating near-simultaneous delivery). Otherwise, the attempt was retried. This acceptance–retry policy was tested in two RF environments (quiet gym, congested hall) and motivates the conservative inter-node term we propagate for section times (see Section 4.4).

End-to-end (T-test workflow). Finally, we validated the complete workflow across the three venues used in this study: laboratory shakedown, entry-hall pilot, gym deployment (real-world conditions). Each trial began with node discovery and sync, followed by execution of the left-side Agility T-test layout (Figure 8). Quality control included: (i) internal consistency checks (sum of section times vs. total time from the start/finish gate), (ii) visual alignment of IMU bursts with gate crossings on the server UI, (iii) trial-level flags for atypical packets or missed replies, and (iv) manual time measurement with a stopwatch. Because timestamps are generated at the edge (ISR), measured network and processing latencies affect throughput and visualization but not timing accuracy. The laboratory shakedown and entry-hall pilot validation were conducted by the authors, while the gym validation was performed with the help of 13 cadets from the Slovenian men's cadet volleyball team, each completing two trials. We emphasize again that the measurements were intended solely for validating the system under real-world conditions, not for assessing the athletes' abilities.

Together, these procedures verify that per-event stamping and intra-device timing behave as expected on the bench, that local clocks remain stable over the durations of interest, that the wireless sync protocol provides an explicit and enforceable quality threshold, and that the full system yields coherent total and section times with aligned kinematic signals in realistic field conditions. Quantitative outcomes referenced above are reported in Sections 4.2–4.5.

5 Discussion

The results confirm that a low-cost, modular system combining infrared gates with a body-worn IMU can achieve timing accuracy sufficient for field-based agility assessment. Device-level uncertainty is dominated by the IR receiver's processing delay and ISR latency, yielding a per-event timestamp error of 0.54 ms ± 0.14 ms (latency ± uncertainty). This translates into a total-time error below 1 ms for trials lasting 10–20 s, which is well within the requirements of standard agility protocols and clearly superior to manual stopwatch timing. It also satisfies sports measurement precision requirements, which are typically set at 0.01 s [2].

Integrating gate events with IMU signals extends beyond conventional timing by enabling interpretation of how performance is achieved. Binding IMU streams to IR events reduces segmentation ambiguity and supports extraction of kinematic markers such as braking and re-acceleration, complementing total and split times. This approach is consistent with recent studies that highlight the utility of IMUs for COD tasks, particularly in the sagittal plane [4]–[9]. Sagittal-plane COD is a core component of real-world agility, so agility tests that meaningfully stress sagittal braking and re-acceleration provide more valid, sport-relevant assessments of an athlete's ability to change speed and direction under realistic conditions.

The main limitation arises from inter-node synchronization in wireless conditions. In favorable RF environments, synchronization spreads remained below 55 µs, but congestion increased jitter and required retries, leading us to conservatively report 15 ms ± 10 ms for section times across gates. It should be noted, that our system is specifically designed for sports halls, where the T-test is typically conducted and where RF conditions are favorable. This positions our approach between NTP-level accuracy and hardware-assisted PTP, while remaining deployable with of-the-shelf Wi-Fi hardware [10], [11], [13].

For practical deployment, several recommendations emerge: stable access point hardware with a wired server connection, consistent beam height and alignment, reliable and consistent body placement of the IMU, and reliance on a watch-crystal time base to bound drift. These practices improve robustness across venues and align with known sources of variability in photocell and IMU-based systems [3]–[7], [21], [22].

Limitations include the reliance on commodity Wi-Fi without hardware timestamping, which constrains synchronization in noisy environments, and the plane-specific accuracy of IMU kinematics reported in the literature [6], [7], and [9].

Beyond controlled laboratory validation, the presented system can be directly applied in sports science and coaching environments for performance assessment, return-to-play testing, and individualized training monitoring. The modular, wireless design makes it suitable for team sports agility drills, rehabilitation progress tracking, and educational use in biomechanics or embedded systems courses. Because the setup requires only a laptop, access point, and portable sensor units, it can also serve as a mobile testing kit for field conditions where commercial optical timing systems are impractical or cost-prohibitive.

In practical terms, the system offers coaches and sports scientists a portable and low-cost alternative to commercial timing systems, providing sub-millisecond accuracy and kinematic insight in everyday training environments. Its modular design and reliance on standard Wi-Fi hardware allow rapid setup and easy adaptation to different sport-specific drills, thereby bridging the gap between laboratory instrumentation and field practice.

6 Conclusions

We presented a wireless, modular measurement system that fuses infrared timing gates with a body-worn IMU for precise, field-ready agility assessment. Device-level total-time errors are below 1 ms over 10–20 s trials, meeting practical requirements for sports testing while preserving a simple, deployable workflow.

By combining gate events with IMU signals, the system provides explanatory value beyond total or split times: aligned kinematic waveforms capture braking, change-of-direction, and re-acceleration phases, supporting technique-aware feedback. For section times across gates, uncertainty is dominated by inter-node synchronization; this term is explicitly quantified to ensure transparent interpretation.

Future work will focus on (i) replacing or augmenting the AP-based synchronization with a dedicated radio channel or hybrid time-sync method to reduce inter-node error, (ii) expanding analytics toward automatic phase classification and asymmetry indices using synchronized IMU signals, and (iii) optional integration with indoor positioning technologies such as UWB for spatial trajectory analysis.

7 Acknowledgments

This work was supported in part by the Slovenian Research and Innovation Agency within the research program ICT4QoL-Information and Communications Technologies for Quality of Life (research core funding no. P2-0246).

8 Conflict of Interest

The authors declare no conflict of interest. The manufacturers of the equipment referenced in this work had no role in the study design; in the collection, analyses, or interpretation of data; in the writing of the manuscript; or in the decision to publish the results.

9 References

[1] K. Pauole, K. Madole, J. Garhammer, M. Lacourse, and R. Rozenek, "Reliability and validity of the T-test as a measure of agility, leg power, and leg speed in college-aged men and women," Journal of Strength and Conditioning Research, vol. 14, no. 4, pp. 443–450, Nov. 2000, doi: 10.1519/00124278-200011000-00012.

[2] R. K. Hetzler, C. D. Stickley, K. M. Lundquist, and I. F. Kimura, "Reliability and accuracy of handheld stopwatches compared with electronic timing in measuring sprint performance," Journal of Strength and Conditioning Research, vol. 22, no. 6, pp. 1969–1976, Nov. 2008, doi: 10.1519/JSC.0b013e318185f36c.

[3] L. Villalón-Gasch, J. M. Jiménez-Olmedo, A. Penichet-Tomas, and S. Sebastia-Amat, "Concurrent validity and reliability of Chronojump photocell in the acceleration phase of linear speed test," Applied Sciences*, vol. 15, no. 16, Art. no. 8852, Aug. 2025.

[4] A.-M. Alanen, A.-M. Räisänen, L. C. Benson, and K. Pasanen, "The use of inertial measurement units for analyzing change of direction movement in sports: A scoping review," International Journal of Sports Science & Coaching, 2021, doi: 10.1177/17479541211003064.

[5] S. Apte, H. Karami, C. Vallat, V. Gremeaux, and K. Aminian, "In-field assessment of change-of-direction ability with a single wearable sensor," Scientific Reports, vol. 13, Art. no. 4518, Mar. 2023, doi: 10.1038/s41598-023-30773-y.

[6] L. Wolski, M. Halaki, C. E. Hiller, E. Pappas, and A. Fong Yan, "Validity of an Inertial Measurement Unit System to Measure Lower Limb Kinematics at Point of Contact during Incremental High-Speed Running," Sensors, vol. 24, no. 17, 5718, Sept. 2024, doi: 10.3390/s24175718.

[7] E. M. Nijmeijer, P. H. Heuvelmans, et al., "Concurrent validation of the Xsens IMU system of lower-body kinematics in jump-landing and change-of-direction tasks," Journal of Biomechanics, vol. 154, 2023.

[8] N. Myhill, D. Weaving, M. Robinson, S. Barrett, and S. Emmonds, "Concurrent validity and between-unit reliability of a foot-mounted inertial measurement unit to measure velocity during team sport activity," Science and Medicine in Football, vol. 8, no. 4, pp. 308–316, 2024, doi: 10.1080/24733938.2023.2237493.

[9] F. Bertozzi, C. Brunetti, P. Maver, M. Palombi, M. Santini, M. Galli, and M. Tarabini, "Concurrent validity of IMU and phone-based markerless systems for lower-limb kinematics during cognitively-challenging landing tasks," Journal of Biomechanics, Aug. 2025, online ahead of print, doi: 10.1016/j.jbiomech.2025.112883.

[10] S. Puckett and E. Jovanov, "ecoSync: An Energy-Efficient Clock Discipline Data Synchronization in Wi-Fi IoMT Systems," Electronics, vol. 12, no. 20, 4226, Oct. 2023, doi: 10.3390/electronics12204226.

[11] P. Chen and Z. Yang, "Understanding Precision Time Protocol in Today's Wi-Fi Networks: A Measurement Study," in Proc. USENIX ATC, Jul. 2021, pp. 597–610.

[12] M. Altet et al., "UWB-Based Real-Time Indoor Positioning Systems: A Comprehensive Review," Applied Sciences, vol. 14, no. 23, 11005, 2024, doi: 10.3390/app142311005.

[13] D. L. Mills, J. Martin, J. Burbank, and W. Kasch, "Network Time Protocol Version 4: Protocol and Algorithms Specification," RFC 5905, Jun. 2010, doi: 10.17487/RFC5905.

[14] E. Keš, Senzorski sistem za ocenjevanje fizičnih sposobnosti v športu (magistrsko delo), Univerza v Ljubljani, Fakulteta za elektrotehniko, 2020. Online: https://repozitorij.uni-lj.si/IzpisGradiva.php?id=121709

[15] Adafruit Industries, "Feather M0 Wi-Fi – ATSAMD21 + ATWINC1500 (Product 3010)," product page, accessed Aug. 22, 2025. Online: https://www.adafruit.com/product/3010

[16] Microchip Technology Inc., "SAM D21/DA1 Family Data Sheet," DS40001882 (latest rev.), accessed Aug. 22, 2025. Online: https://ww1.microchip.com/downloads/aemDocuments/documents/MCU32/ProductDocuments/DataSheets/SAM-D21-DA1-Family-Data-Sheet-DS40001882.pdf

[17] Microchip Technology Inc., "ATWINC15x0-MR210xB IEEE® 802.11 b/g/n SmartConnect IoT Module," DS70005304 (rev. F or latest), accessed Aug. 22, 2025. Online: https://ww1.microchip.com/downloads/aemDocuments/documents/WSG/ProductDocuments/DataSheets/ATWINC15x0-MR210xB-Wi-Fi-Module-Data-Sheet-DS70005304.pdf

[18] Sharp Corporation, "IS471F: OPIC Light Detector with Built-in Signal Processing Circuit," datasheet, accessed Aug. 22, 2025. Online: https://mm.digikey.com/Volume0/opasdata/d220001/medias/docus/987/IS471F.pdf

[19] Vishay Semiconductors, "TSAL6200: High-Power Infrared Emitting Diode, 940 nm," datasheet, accessed Aug. 22, 2025. Online: https://www.vishay.com/doc/81010/tsal6200.pdf

[20] SICK AG, "P250 Reflector—Reflectors and Optics," datasheet 5304812, accessed Aug. 22, 2025. Online: https://www.sick.com/media/pdf/4/94/694/dataSheet_P250_5304812_en.pdf

[21] STMicroelectronics, "LSM6DS33: iNEMO inertial module—3D accelerometer and 3D gyroscope," datasheet, accessed Aug. 22, 2025. Online: https://www.pololu.com/file/0J1087/LSM6DS33.pdf

[22] Bosch Sensortec, "BNO055: Intelligent 9-axis absolute orientation sensor," datasheet (rev. 1.2), accessed Aug. 22, 2025. Online: https://cdn-shop.adafruit.com/datasheets/BST_BNO055_DS000_12.pdf

Arrived: 03.10.2025
Accepted: 20.11.2025